



**Scalable, Room Temperature, and Water-based Synthesis of Functionalized Zirconium-based Metal-Organic Frameworks for Toxic Chemical Removal**

Journal:	<i>CrystEngComm</i>
Manuscript ID	CE-ART-02-2019-000213
Article Type:	Paper
Date Submitted by the Author:	14-Feb-2019
Complete List of Authors:	Chen, Zhijie; Northwestern University, Chemistry Farha, Omar; Northwestern University, Department of Chemistry Wang, Xingjie; Northwestern University, Chemistry Noh, Hyunho; Northwestern University Ayoub, Ghada; McGill University, Department of Chemistry Peterson, Gregory; Edgewood Chemical Biological Center, Islamoglu, Timur; Northwestern University, Department of Chemistry Buru, Cassandra; Northwestern University, Chemistry

## ARTICLE

# Scalable, Room Temperature, and Water-based Synthesis of Functionalized Zirconium-based Metal-Organic Frameworks for Toxic Chemical Removal

Cite this: DOI: 10.1039/x0xx00000x

Received 00th January 2012,  
Accepted 00th January 2012

DOI: 10.1039/x0xx00000x

[www.rsc.org/](http://www.rsc.org/)

Zhijie Chen,<sup>a</sup> Xingjie Wang,<sup>a</sup> Hyunho Noh,<sup>a</sup> Ghada Ayoub,<sup>a</sup> Gregory W. Peterson,<sup>b</sup> Cassandra T. Buru,<sup>a</sup> Timur Islamoglu<sup>a</sup> and Omar K. Farha<sup>\*a</sup>

An inexpensive, environmentally benign and scalable strategy was developed to synthesize UiO-66 derivatives in water at room temperature. Particularly, UiO-66-(COOH)<sub>2</sub> with significant amount of missing Zr<sub>6</sub> clusters exhibited comparably high surface area and high pore volume as to the same material synthesized at higher temperatures. The presence of both the Lewis and Brønsted acidic active sites permits the high affinity for ammonia under both dry and humid environments. Additionally, we have developed a synthesis for the hydrophobic analogue, UiO-66-F<sub>4</sub>, which hydrolyzed the hydrophobic VX agent at 50% relative humidity without buffer and bulk water. The scalable synthesis of UiO-66 analogues in water at room temperature makes these materials practical and promising candidates for toxic chemical removal applications.

## 1. Introduction

Metal–organic frameworks (MOFs),<sup>1–6</sup> a class of functional porous hybrid organic-inorganic materials, have been explored in the past two decades for many potential applications such as heterogeneous catalysis,<sup>7–13</sup> water capture,<sup>14–18</sup> large molecule encapsulation,<sup>19–21</sup> gas storage and separations.<sup>22–28</sup> The atomically precise tunability of framework structures allows for the design and synthesis of MOFs for targeted applications.<sup>29–37</sup> Due to this unique control over MOFs compared to those of traditional porous counterparts such as activated carbon and zeolites, MOFs have received interest not only from academia but also from several industries, which are seeking to commercialize MOF materials.<sup>38</sup> However, the scalable synthesis of functional MOFs in an environmentally and economically viable fashion still needs to be explored.<sup>39</sup> To this end, the synthesis of MOFs in an aqueous environment under ambient conditions has attracted great attention.<sup>40, 41</sup> Room temperature (RT) syntheses of MOFs in water: 1) decreases the cost of production, which is vital for the large-scale applications such as adsorption based separation and storage; 2) increases the safety of operation; 3) reduces the generation of toxic byproducts (i.e. solvents); 4) enables the encapsulation of heat and/or organic solvent-sensitive materials such as enzymes and nanoparticles for specific applications.

Specifically, UiO-66, consisting of hexanuclear oxo-zirconium clusters ( $Zr_6$  nodes) and organic terephthalate ligands, is among the most prevalent MOF since its discovery in 2008,<sup>42</sup> due to the high thermal and hydrolytic stability, as well as, the ease of functionalization and isorecticular structural tuning.<sup>43–48</sup> Most reported UiO-66 analogues are synthesized via solvothermal crystallization in toxic, flammable and expensive organic solvents such as *N,N*-dimethylformamide (DMF)<sup>42</sup> or *N,N*-dimethylacetamide (DMA)<sup>49</sup> at high temperature (i.e. 120 °C), which requires intensive energy input. Recently, we have demonstrated the viability of RT syntheses of UiO-66 and NU-901, another  $Zr_6$ -based MOF with tetratopic linkers, using organic solvents.<sup>50, 51</sup> The safe and low-cost aqueous syntheses have recently been explored in the construction of UiO-type MOFs; although, they generally require high temperatures.<sup>44, 52–57</sup>

Among many, one application of MOFs that would greatly benefit from a scalable synthesis under environmentally benign conditions is the use of MOFs as solid sorbents and/or catalysts for toxic chemicals such as ammonia and nerve agents. Ammonia ( $NH_3$ ) is one of the most produced industrial gases due to its high utility in large-scale applications like in the manufacture of fertilizers, medicines, and explosives.<sup>58–60</sup> Efficient sorbent materials for ammonia are required for personal protective equipment and industrial air purification due to its high toxicity.<sup>35, 61</sup> However, current chemical filters are generally unselective and inefficient, so there is a pressing need to improve current technology for selective and high capacity sorbents. Porous sorbents with Lewis or Brønsted acidic sites are reported to be efficient in the capture of basic ammonia.<sup>62–67</sup> Nevertheless, sorbents

with both accessible Lewis and Brønsted acidic sites are still rare and could provide enhanced efficiency.

On the other hand, the very hydrophobic chemical warfare agent VX (O-ethyl S-[2-(diisopropylamino)ethyl] methylphosphonothioate) consists of phosphonate linkages and is one of the most toxic chemicals to humankind.<sup>68, 69</sup> One potential effective way to detoxify VX is to use porous MOF sorbents with both accessible Lewis acidic sites and hydrophobic pore environments to hydrolyze the reactive P-S bond; however, the solid-state reactivity of MOFs for the hydrolysis of liquid drops of VX has yet to be explored.<sup>70</sup> Herein, we report benign reaction conditions for the synthesis of two UiO-66 analogues, including UiO-66-(COOH)<sub>2</sub> (1,2,4,5-benzenetetracarboxylic acid; H<sub>2</sub>BTEC) and UiO-66-F<sub>4</sub> (tetrafluoroterephthalic acid; H<sub>2</sub>BDC-F<sub>4</sub>), by utilizing zirconium(IV) oxynitrate ( $ZrO(NO_3)_2$ ) as the metal source with trifluoroacetic acid (TFA) or acetic acid (AA) as the modulator in water (**Fig. 1A**). The UiO-66-(COOH)<sub>2</sub> and UiO-66-F<sub>4</sub> were found to contain a large amount of missing cluster defects as revealed by powder X-ray diffraction (PXRD) patterns, density functional theory (DFT) pore-size distributions obtained from N<sub>2</sub> isotherms and thermogravimetric analysis (TGA). Moreover, the preparation of UiO-66-(COOH)<sub>2</sub> can be simply and reliably scaled up from 30 mg to 20 g. The scalable synthesis further marks these materials practical and promising candidates for toxic chemical removal applications such as ammonia capture and nerve agent VX detoxification.

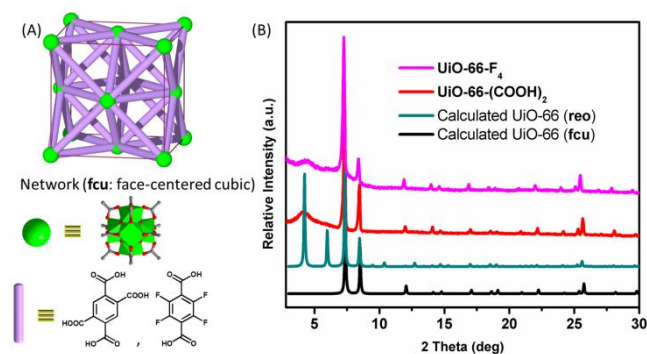


**Fig. 1.** (A) Illustration of the topological network of idealized UiO-66 analogues: face-centered cubic (fcc) net; the green ball represents the  $Zr_6$  node and lavender stick represents the ditopic benzenedicarboxylic acid linker. (B) The comparison of experimental PXRD patterns with the calculated PXRD patterns from the UiO-66 (fcc) and UiO-66 (reo), the most representative missing cluster structure of UiO-66. Atom color scheme: C, grey; Zr, green polyhedron; O, red. H atoms are omitted for clarity.

## 2. Results and discussion

UiO-66-(COOH)<sub>2</sub> was chosen as the first target due to the high solubility of the H<sub>2</sub>BTEC linker in water at RT. The two additional carboxylic acid functional groups in the linker has enabled this MOF to be applied in carbon dioxide capture,<sup>44, 52</sup> water sorption,<sup>52</sup> ammonia removal,<sup>67</sup> and proton conductivity.<sup>71</sup> However, to the best of our knowledge, there is no report of the aqueous synthesis of UiO-66-(COOH)<sub>2</sub> at room temperature. In this work, zirconium (IV) oxynitrate ( $ZrO(NO_3)_2$ ) was selected as the metal source due to its high

water solubility and the less corrosive nature of nitrate salts compared to chloride salts. The initial trial with  $\text{ZrO}(\text{NO}_3)_2$  and  $\text{H}_2\text{BTEC}$  in water under continuous stirring with AA as the modulator (water/AA (v/v) = 6/1) was unsuccessful, and an unknown amorphous gel was obtained after 2 days (**Fig. S3**). We suspected a stronger acid is needed to modulate the formation of crystalline MOFs, and therefore, we employed TFA as modulator ( $\text{p}K_a$  of TFA [0.23] is less than AA [4.76]). The use of TFA as a modulator (water/TFA (v/v) = 6/1) under the same conditions led to the successful crystallization of  $\text{UiO-66}(\text{COOH})_2$  at RT (**Table 1** and **Table S1**). Amorphous powders were formed by using lower concentration of TFA (water/TFA (v/v) = 30/1) under the same conditions, which suggests that the TFA concentration is critical for MOF crystallization. Notably, increasing the amount of AA (water/AA (v/v) = 1/1) still yielded the white amorphous powders, which highlights the importance of TFA in the synthesis of  $\text{UiO-66}(\text{COOH})_2$  at room temperature in water.

The phase purity of the bulk crystalline  $\text{UiO-66}(\text{COOH})_2$  was confirmed by comparing the as-synthesized PXRD patterns with the simulated PXRD pattern of the idealized  $\text{UiO-66}$  crystal structure possessing the 12-connected **fcu** topology (**Fig. 1B**). A broad peak at  $4.2^\circ$  was also observed for the  $\text{UiO-66}(\text{COOH})_2$ , indicating the presence of ordered missing cluster defects within the MOF structure.<sup>72</sup> This broad peak corresponds to the Bragg peak reflected from the (100) plane of the proposed missing cluster defect of  $\text{UiO-66}$  structures based on the 3-periodic 8-connected **reo** net.<sup>72</sup>  $\text{N}_2$  adsorption-desorption measurements revealed the experimental total pore volume at  $P/P_0 = 0.8$  and the apparent Brunauer–Emmett–Teller (BET) area of  $\text{UiO-66}(\text{COOH})_2$  were estimated to be  $0.37 \text{ cm}^3 \cdot \text{g}^{-1}$  and  $890 \text{ m}^2 \cdot \text{g}^{-1}$ , respectively (**Fig. 2, top**). Moreover, the non-local density functional theory (NLDFT) pore size distribution indicated a notable, extra pore centered at  $\sim 1.6 \text{ nm}$ , in addition to the main pore correlated to the parent perfect  $\text{UiO-66}$  (**fcu**) structure ( $1.1 \text{ nm}$ ) (**Fig. 2, bottom**). This confirms the presence of a significant amount of missing cluster defects in the  $\text{UiO-66}(\text{COOH})_2$ . Additionally, there is no  $\text{ZrO}_2$  phase

observed from PXRD ( $2\theta$  from  $1$  to  $80^\circ$ ), confirming the phase purity of  $\text{UiO-66}(\text{COOH})_2$  (**Fig. S4**), which is supported by  $\text{N}_2$  sorption and SEM images (**Fig. S5**)

The TGA plot of  $\text{UiO-66}(\text{COOH})_2$  under continuous air flow indicated that the framework is stable up to  $\sim 350^\circ\text{C}$  (**Fig. S6**). The number of linkers per  $\text{Zr}_6$  node was estimated to be about 3.7 based on the TGA plot, indicating the highly defective nature of this material. The band at  $3631 \text{ cm}^{-1}$  in diffuse reflectance infrared Fourier transform spectroscopy (DRIFTS) spectrum could be assigned to the bridging  $\mu_3\text{-OH}$  groups in  $\text{Zr}_6$  nodes which further confirms the  $\text{UiO-66}$  structure (**Fig. S7**).<sup>73</sup>

The procedure developed here for  $\text{UiO-66}(\text{COOH})_2$  can easily be scaled up to yield 20 g of MOFs (**Fig. S1**). The phase purity and porosity are retained in the scaled-up batch (**Fig. S2** and **S8**), suggesting that this synthetic route can be applied to the large-scale production of MOF sorbents.

To tune the defect density in  $\text{UiO-66}(\text{COOH})_2$  based on the aqueous synthesis, we performed the same reaction at different temperatures, including  $40$ ,  $80$  and  $100^\circ\text{C}$  (reflux). The resulting PXRD patterns of  $\text{UiO-66}(\text{COOH})_2$ , after normalizing the (111) Bragg peak at  $2\theta = 7.4^\circ$ , showed reduced intensity of the broad peak at  $2\theta = 4.2^\circ$ . This indicates that the  $\text{UiO-66}(\text{COOH})_2$  synthesized at  $100^\circ\text{C}$  ( $\text{UiO-66}(\text{COOH})_2\text{-}100^\circ\text{C}$ ) has fewer missing cluster defects compared to the materials synthesized at the lower temperatures. The comparison of  $\text{N}_2$  sorption isotherms at  $77 \text{ K}$  of  $\text{UiO-66}(\text{COOH})_2$  synthesized at different temperatures exhibited that  $\text{UiO-66}(\text{COOH})_2\text{-}100^\circ\text{C}$  has the lowest experimental total pore volume at  $P/P_0 = 0.8$  of  $0.33 \text{ cm}^3 \cdot \text{g}^{-1}$  and the lowest estimated apparent BET area of ca.  $820 \text{ m}^2 \cdot \text{g}^{-1}$  (**Fig. S9-10** and **Table S2**). The NLDFT pore size distribution displayed a much smaller shoulder centered at  $\sim 1.8 \text{ nm}$  compared to when the material was synthesized at lower temperatures (**Fig. S10**) which is expected due to the presence of less defects. However, there are still some defects in the  $\text{UiO-66}(\text{COOH})_2$  structure when synthesized under reflux. We note that similar temperature-defect density correlation has also been observed in organic media.<sup>50</sup>

**Table 1. Summary of the water-based syntheses of  $\text{UiO-66}$  analogues.**

MOFs	Metal Source	Modulator	Water/Modulator (v/v)	Temperature	BET surface area ( $\text{m}^2 \cdot \text{g}^{-1}$ ) <sup>a</sup>
$\text{UiO-66}(\text{COOH})_2$	$\text{ZrO}(\text{NO}_3)_2$	TFA <sup>b</sup>	6/1	RT	890
$\text{UiO-66-F}_4$	$\text{ZrO}(\text{NO}_3)_2$	AA <sup>c</sup>	8/1	RT	690

<sup>a</sup> Calculated from experimental  $\text{N}_2$  adsorption isotherms at  $77 \text{ K}$ . <sup>b</sup> TFA = trifluoroacetic acid. <sup>c</sup> AA = acetic acid.

## ARTICLE

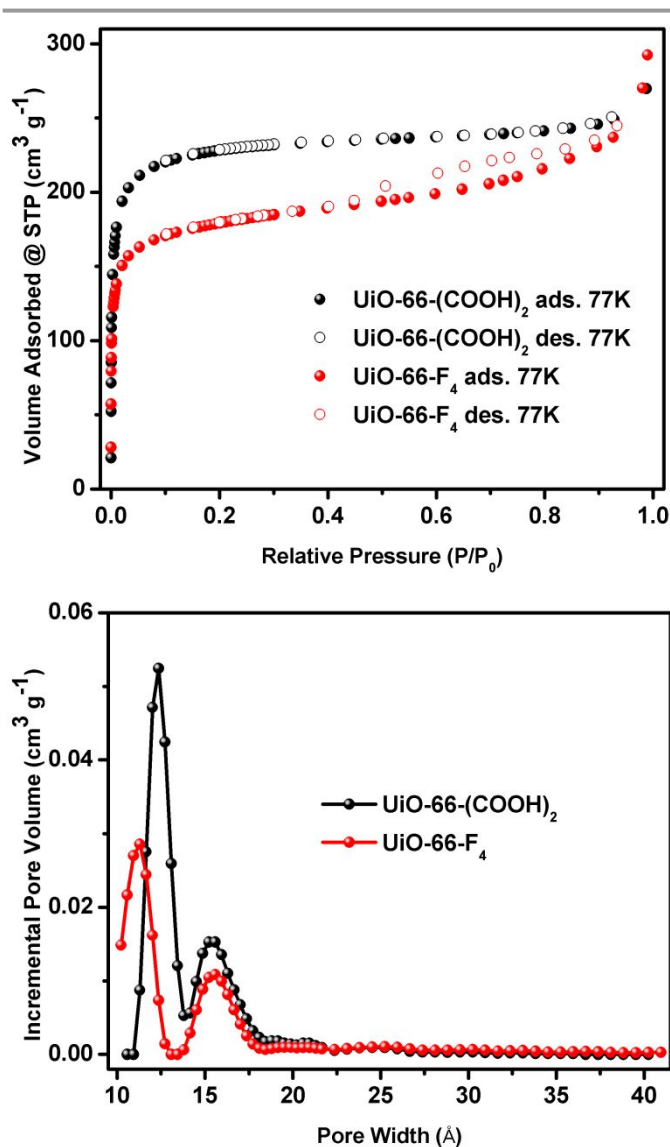


**Fig. 2.** N<sub>2</sub> sorption isotherms at 77 K (top) and non-local density functional theory (NLDFT) pore size distribution (bottom) of UiO-66-(COOH)<sub>2</sub> and UiO-66-F<sub>4</sub>.

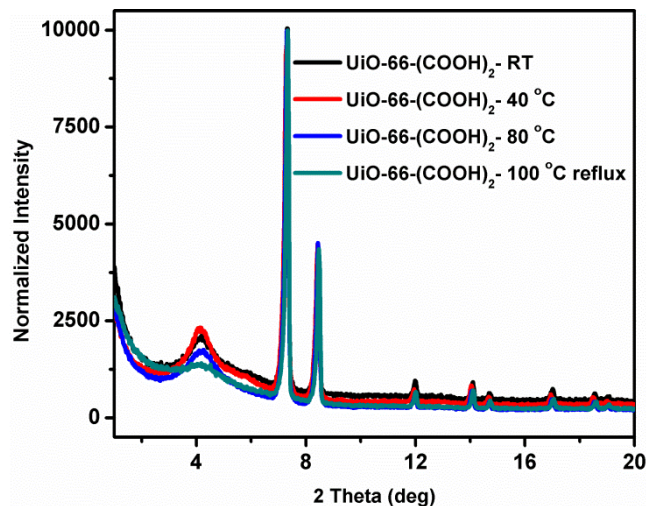


**Fig. 3.** PXRD patterns of UiO-66-(COOH)<sub>2</sub> from the syntheses based on the different temperatures, after normalizing the (111) Bragg peak at 2 theta = 7.4° of UiO-66-(COOH)<sub>2</sub>.

To illustrate the versatility of this synthetic strategy, UiO-66-F<sub>4</sub> was also synthesized in water at RT by combining ZrO(NO<sub>3</sub>)<sub>2</sub> with H<sub>2</sub>BDC-F<sub>4</sub>, employing acetic acid as a modulator. The PXRD patterns of UiO-66-F<sub>4</sub> confirmed the phase purity of these materials (**Fig. 1B**). TGA plot indicated that this framework is stable up to about 350 °C (**Fig. S6**). N<sub>2</sub> adsorption isotherm at 77 K of UiO-66-F<sub>4</sub> revealed that the experimental total pore volumes at P/P<sub>0</sub> = 0.8 are 0.33 cm<sup>3</sup>·g<sup>-1</sup>, and the estimated apparent BET areas are ca. 690 m<sup>2</sup>·g<sup>-1</sup> (**Fig. 2** and **Table S3**). From the NLDFT pore size distribution, UiO-66-F<sub>4</sub> has additional pores centered about ~1.6 nm, which indicates a highly defective structure.

To explore the functionality of UiO-66-(COOH)<sub>2</sub> which benefits from both the Brønsted acidic active sites due to free carboxylic acids and Lewis acidic active sites due to defective structures, NH<sub>3</sub> breakthrough experiments using a micro-breakthrough system were performed under humid and dry conditions (**Fig. 4**).<sup>60, 74, 75</sup> The ammonia capacity was determined by integrating the breakthrough curves.<sup>75</sup> Under dry conditions, UiO-66-(COOH)<sub>2</sub> showed a moderate ammonia capacity of ~2.4 mol/kg; while under humid conditions, the MOF displayed enhanced ammonia capacity of ~5.6 mol/kg. We attributed this phenomenon to the presence of both accessible Brønsted and Lewis acidic active sites inside UiO-66-(COOH)<sub>2</sub> due to their defective nature. Enhanced NH<sub>3</sub> uptake in a porous material under humid conditions has been previously attributed to the solubility of NH<sub>3</sub> in water presented inside the pores.<sup>61</sup> We observed formation of amides during the NH<sub>3</sub> adsorption as illustrated by the appearance of shoulder

$\sim 1650\text{ cm}^{-1}$  while the band at  $1700\text{ cm}^{-1}$  due to free carboxylate C=O stretching was diminishing in the attenuated total reflectance Fourier transform infrared (ATR-FTIR) spectra. The comparison of the  $\text{NH}_3$  breakthrough performance of UiO-66-(COOH) $_2$  with prototype UiO-66 further demonstrates the importance of the free carboxylic acid sites for the  $\text{NH}_3$  capture. The UiO-66-(COOH) $_2$  with lower amounts of defects (i.e. UiO-66-(COOH) $_2$ -100 °C or UiO-66-(COOH) $_2$ \_low defect), shows lower ammonia capacity of 1.6 mol/kg and 2.6 mol/kg, respectively, which is the consequence of the lower surface area and fewer missing cluster defective sites (Fig. S11-14). This demonstrates that there is a trade-off between incorporating of more adsorption sites (free carboxylic acid in this case) and lowering the pore volume of the sorbent, which is an important consideration when designing next generation sorbents.

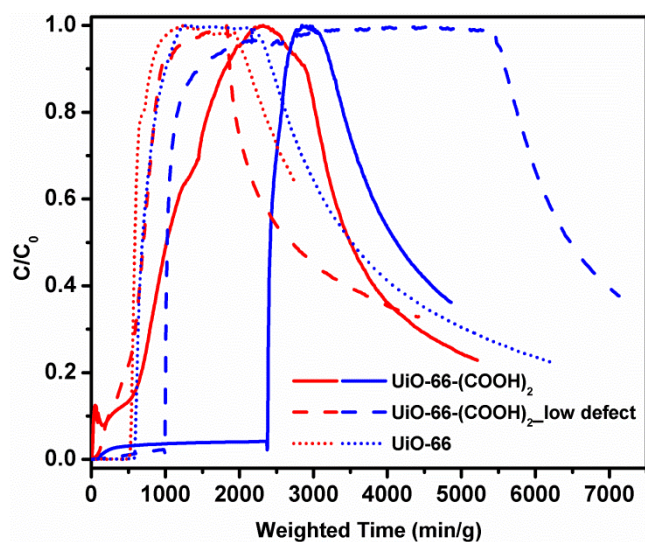


**Fig. 4.**  $\text{NH}_3$  microbreakthrough curves under dry (red) and humid (blue) conditions.

Porous materials for filtration and detoxification of chemical warfare agents, such as VX, Sarin, and Soman, are urgently needed for use both in the field and in the bulk decontamination of stockpiles.<sup>35, 76</sup> Particularly, due to the hydrophobicity of VX, we proposed a porous catalyst with both accessible Lewis acidic sites and hydrophobic pore environments could effectively hydrolyze VX under certain RH. In this regard, UiO-66-F $_4$  was selected to study the hydrolysis of VX under 50% RH, thanks to the presence of fluorinated linkers, which facilitates the adsorption of the hydrophobic VX agent. Previously, Zr $_6$ -based MOFs such as NU-1000 and UiO-67 have been reported to selectively hydrolyze VX via cleavage of the P-S bond to the nontoxic products EMPA (ethyl methylphosphonic acid) and DESH [2-(diisopropylamino)ethanethiol] in buffer and liquid water (Fig. 5A).<sup>8, 70</sup> However, the study of the hydrolysis of VX without the use of bulk water and buffer, a more practical condition for chemical filtration and detoxification, has yet to be reported. Here the hydrolysis of VX by UiO-66-F $_4$  was conducted under 50% RH, and the conversion was calculated by comparing the

integrated  $^{31}\text{P}$  peaks based on  $^{31}\text{P}$  solid state magic angle spinning nuclear magnetic resonance (MAS NMR) spectra for VX to that of nontoxic ethyl methylphosphonate (EMPA) anion (Fig. 5B and Fig. S15).<sup>77</sup> The reaction half-life ( $t_{1/2}$ ) of UiO-66-F $_4$  was calculated to be  $\sim 108$  min via plotting the natural log of the concentration versus time and assuming the hydrolysis as a pseudo-first-order process. Notably, only a very small amount of the toxic byproduct EA-2192 [S-2-(diisopropylamino)ethyl O-hydrogen methylphosphonothioate] by hydrolysis of the P-O bond was observed as indicated by  $^{31}\text{P}$  NMR spectra (Fig. S15). This study here represents a practical and important step towards detoxification of nerve agent VX under realistic conditions without the use of buffer and the bulk water.

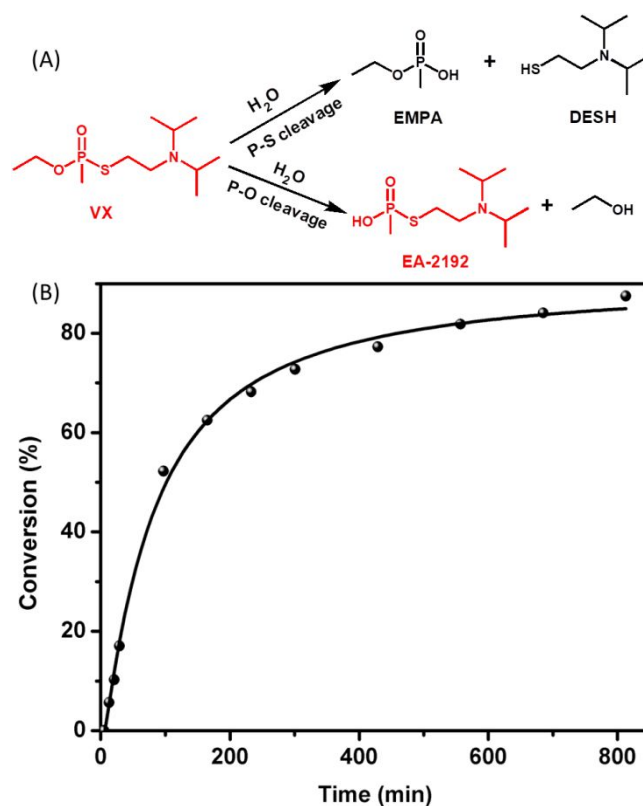


**Fig. 5.** (A) Stoichiometric hydrolysis reactions of O-ethyl S-[2-(diisopropylamino)ethyl] methylphosphonothioate (VX). (B) Hydrolysis profile of VX to EMPA in the presence of UiO-66-F $_4$  under 50% RH.

### 3. Conclusions

In conclusion, we have developed an inexpensive and scalable synthetic strategy for the aqueous synthesis of UiO-66 MOFs at room temperature. UiO-66-(COOH) $_2$  with large amount of missing cluster defects exhibits attractive performance for the ammonia capture under both dry and humid conditions. The scalable synthesis of UiO-66-(COOH) $_2$  further makes this material a promising solid porous sorbent for the practical use in ammonia capture for personal protective equipment and industrial air purification systems. Hydrophobic pores and Lewis acidic Zr-nodes of UiO-66-F $_4$  facilitated the adsorption

followed by the selective hydrolysis of hydrophobic nerve agent VX with under 50% RH. These promising results pave the way for MOFs to be utilized as porous sorbents and catalysts for decontamination of toxic chemicals under real-world conditions.

## Acknowledgements

O.K.F. gratefully acknowledges STIR (W911NF-18-1-0050) for the financial support. H.N. gratefully acknowledges support from the Ryan Fellowship program of the Northwestern University International Institute of Nanotechnology. This work made use of the EPIC facility of Northwestern University's NUANCE Center, which has received support from the Soft and Hybrid Nanotechnology Experimental (SHyNE) Resource (NSF NNCI-1542205); the MRSEC program (NSF DMR-1720139) at the Materials Research Center; the International Institute for Nanotechnology (IIN); the Keck Foundation; and the State of Illinois, through the IIN. This work made use of the IMSERC at Northwestern University, which has received support from the NSF (CHE-1048773 and DMR0521267); Soft and Hybrid Nanotechnology Experimental (SHyNE) Resource (NSF NNCI-1542205); the State of Illinois and International Institute for Nanotechnology (IIN). X.W. acknowledges support from China Scholarship Council (CSC) during his visit to Northwestern University. We acknowledged Amedeo Napolitano, Morgan Hall, and Eric Bruni for measuring data.

## Notes and references

<sup>a</sup>Department of Chemistry and International Institute of Nanotechnology, Northwestern University, 2145 Sheridan Road, Evanston, Illinois 60208, United States. E-mail: o-farha@northwestern.edu

<sup>b</sup>Edgewood Chemical Biological Center, U.S. Army Research, Development, and Engineering Command, 5183 Blackhawk Road, Aberdeen Proving Ground, Maryland 21010, United States

The authors declare no competing financial interest.

† Electronic Supplementary Information (ESI) available: the synthetic procedures of MOF materials, additional adsorption figures, TGA curves, SEM images, PXRD plots, and <sup>31</sup>P MAS NMR spectra (PDF).

- H. Furukawa, K. E. Cordova, M. O'Keeffe and O. M. Yaghi, *Science*, 2013, **341**, 1230444.
- G. Ferey, *Chem. Soc. Rev.*, 2008, **37**, 191-214.
- S. Kitagawa, R. Kitaura and S. Noro, *Angew. Chem. Int. Ed.*, 2004, **43**, 2334-2375.
- G. K. H. Shimizu, R. Vaidhyanathan and J. M. Taylor, *Chem. Soc. Rev.*, 2009, **38**, 1430-1449.
- T. D. Bennett and S. Horike, *Nat Rev Mater.*, 2018, **3**, 431-440.
- Z. Chen, S. L. Hanna, L. R. Redfern, D. Alezi, T. Islamoglu and O. K. Farha, *Coord. Chem. Rev.*, 2019, **386**, 32-49.
- J. Lee, O. K. Farha, J. Roberts, K. A. Scheidt, S. T. Nguyen and J. T. Hupp, *Chem. Soc. Rev.*, 2009, **38**, 1450-1459.
- J. E. Mondloch, M. J. Katz, W. C. Isley Iii, P. Ghosh, P. Liao, W. Bury, G. W. Wagner, M. G. Hall, J. B. DeCoste, G. W. Peterson, R. Q. Snurr, C. J. Cramer, J. T. Hupp and O. K. Farha, *Nat. Mater.*, 2015, **14**, 512-516.
- A. W. Peters, Z. Li, O. K. Farha and J. T. Hupp, *ACS Nano*, 2015, **9**, 8484-8490.
- J.-S. Qin, S. Yuan, C. Lollar, J. Pang, A. Alsalmeh and H.-C. Zhou, *Chem. Commun.*, 2018, **54**, 4231-4249.
- M. D. Korzyński, D. F. Consoli, S. Zhang, Y. Román-Leshkov and M. Dincă, *J. Am. Chem. Soc.*, 2018, **140**, 6956-6960.
- A. Lin, A. A. Ibrahim, P. Arab, H. M. El-Kaderi and M. S. El-Shall, *ACS Appl. Mater. Interfaces*, 2017, **9**, 17961-17968.
- Z. Chen, T. Islamoglu and O. K. Farha, *ACS Appl. Nano Mater.*, 2019, DOI: 10.1021/acsanm.8b02292.
- H. Furukawa, F. Gándara, Y.-B. Zhang, J. Jiang, W. L. Queen, M. R. Hudson and O. M. Yaghi, *J. Am. Chem. Soc.*, 2014, **136**, 4369-4381.
- H. Kim, S. Yang, S. R. Rao, S. Narayanan, E. A. Kapustin, H. Furukawa, A. S. Umans, O. M. Yaghi and E. N. Wang, *Science*, 2017, **356**, 430-434.
- A. Cadiau, Y. Belmabkhout, K. Adil, P. M. Bhatt, R. S. Pillai, A. Shkurenko, C. Martineau-Corcus, G. Maurin and M. Eddaoudi, *Science*, 2017, **356**, 731-735.
- A. J. Rieth, S. Yang, E. N. Wang and M. Dincă, *ACS Cent. Sci.*, 2017, **3**, 668-672.
- Z. Chen, P. Li, X. Zhang, P. Li, M. C. Wasson, T. Islamoglu, J. F. Stoddart and O. K. Farha, *J. Am. Chem. Soc.*, 2019, DOI: 10.1021/jacs.8b13710.
- X. Lian, Y. Fang, E. Joseph, Q. Wang, J. Li, S. Banerjee, C. Lollar, X. Wang and H.-C. Zhou, *Chem. Soc. Rev.*, 2017, **46**, 3386-3401.
- P. Li, Q. Chen, T. C. Wang, N. A. Vermeulen, B. L. Mehdi, A. Dohnalkova, N. D. Browning, D. Shen, R. Anderson, D. A. Gómez-Gualdrón, F. M. Cetin, J. Jagiello, A. M. Asiri, J. F. Stoddart and O. K. Farha, *Chem*, 2018, **4**, 1022-1034.
- V. Lykourinou, Y. Chen, X.-S. Wang, L. Meng, T. Hoang, L.-J. Ming, R. L. Musselman and S. Ma, *J. Am. Chem. Soc.*, 2011, **133**, 10382-10385.
- K. Adil, Y. Belmabkhout, R. S. Pillai, A. Cadiau, P. M. Bhatt, A. H. Assen, G. Maurin and M. Eddaoudi, *Chem. Soc. Rev.*, 2017, **46**, 3402-3430.
- B. Li, H.-M. Wen, W. Zhou, Jeff Q. Xu and B. Chen, *Chem*, 2016, **1**, 557-580.
- J. A. Mason, M. Veenstra and J. R. Long, *Chem. Sci.*, 2014, **5**, 32-51.
- Y. Belmabkhout, R. S. Pillai, D. Alezi, O. Shekhah, P. M. Bhatt, Z. Chen, K. Adil, S. Vaesen, G. De Weireld, M. Pang, M. Suetin, A. J. Cairns, V. Solovyeva, A. Shkurenko, O. El Tall, G. Maurin and M. Eddaoudi, *J. Mater. Chem. A*, 2017, **5**, 3293-3303.
- Z. Chen, K. Adil, L. J. Weselinski, Y. Belmabkhout and M. Eddaoudi, *J. Mater. Chem. A*, 2015, **3**, 6276-6281.
- D. S. Sholl and R. P. Lively, *Nature News*, 2016, **532**, 435.
- D. Banerjee, A. J. Cairns, J. Liu, R. K. Motkuri, S. K. Nune, C. A. Fernandez, R. Krishna, D. M. Strachan and P. K. Thallapally, *Acc. Chem. Res.*, 2015, **48**, 211-219.
- O. Shekhah, Y. Belmabkhout, Z. Chen, V. Guillerme, A. Cairns, K. Adil and M. Eddaoudi, *Nat. Commun*, 2014, **5**, 4228.
- Z. Chen, L. J. Weseliński, K. Adil, Y. Belmabkhout, A. Shkurenko, H. Jiang, P. M. Bhatt, V. Guillerme, E. Dauzon,

- D.-X. Xue, M. O’Keeffe and M. Eddaoudi, *J. Am. Chem. Soc.*, 2017, **139**, 3265-3274.
31. J. Liu, J. Ye, Z. Li, K.-i. Otake, Y. Liao, A. W. Peters, H. Noh, D. G. Truhlar, L. Gagliardi, C. J. Cramer, O. K. Farha and J. T. Hupp, *J. Am. Chem. Soc.*, 2018, **140**, 11174-11178.
32. P. Ryan, O. K. Farha, L. J. Broadbelt and R. Q. Snurr, *AIChE J.*, 2010, **57**, 1759-1766.
33. T. Islamoglu, M. A. Ortuño, E. Proussaloglou, A. J. Howarth, N. A. Vermeulen, A. Atilgan, A. M. Asiri, C. J. Cramer and O. K. Farha, *Angew. Chem. Int. Ed.*, 2018, **57**, 1949-1953.
34. Z. Chen, H. Jiang, M. O’Keeffe and M. Eddaoudi, *Faraday Discuss.*, 2017, **201**, 127-143.
35. J. B. DeCoste and G. W. Peterson, *Chem. Rev.*, 2014, **114**, 5695-5727.
36. P. F. Muldoon, C. Liu, C. C. Miller, S. B. Koby, A. Gamble Jarvi, T.-Y. Luo, S. Saxena, M. O’Keeffe and N. L. Rosi, *J. Am. Chem. Soc.*, 2018, **140**, 6194-6198.
37. B. Garai, A. Mallick and R. Banerjee, *Chem. Sci.*, 2016, **7**, 2195-2200.
38. *Nat. Chem.*, 2016, **8**, 987.
39. B. Karadeniz, A. J. Howarth, T. Stolar, T. Islamoglu, I. Dejanović, M. Tireli, M. C. Wasson, S.-Y. Moon, O. K. Farha, T. Friščić and K. Užarević, *ACS Sustain Chem Eng.*, 2018, **6**, 15841-15849.
40. Y. Pan, Y. Liu, G. Zeng, L. Zhao and Z. Lai, *Chem. Commun.*, 2011, **47**, 2071-2073.
41. L. Garzón-Tovar, A. Carné-Sánchez, C. Carbonell, I. Imaz and D. MasPOCH, *J. Mater. Chem. A*, 2015, **3**, 20819-20826.
42. J. H. Cavka, S. Jakobsen, U. Olsbye, N. Guillou, C. Lamberti, S. Bordiga and K. P. Lillerud, *J. Am. Chem. Soc.*, 2008, **130**, 13850-13851.
43. S. J. Garibay and S. M. Cohen, *Chem. Commun.*, 2010, **46**, 7700-7702.
44. Q. Yang, S. Vaesen, F. Ragon, A. D. Wiersum, D. Wu, A. Lago, T. Devic, C. Martineau, F. Taulelle, P. L. Llewellyn, H. Jovic, C. Zhong, C. Serre, G. De Weireld and G. Maurin, *Angew. Chem. Int. Ed.*, 2013, **52**, 10316-10320.
45. T.-F. Liu, D. Feng, Y.-P. Chen, L. Zou, M. Bosch, S. Yuan, Z. Wei, S. Fordham, K. Wang and H.-C. Zhou, *J. Am. Chem. Soc.*, 2015, **137**, 413-419.
46. Y. Bai, Y. Dou, L.-H. Xie, W. Rutledge, J.-R. Li and H.-C. Zhou, *Chem. Soc. Rev.*, 2016, **45**, 2327-2367.
47. Z. Chen, L. Feng, L. Liu, P. M. Bhatt, K. Adil, A. H. Emwas, A. H. Assen, Y. Belmabkhout, Y. Han and M. Eddaoudi, *Langmuir*, 2018, **34**, 14546-14551.
48. R. J. Marshall and R. S. Forgan, *Eur. J. Inorg. Chem.*, 2016, **2016**, 4310-4331.
49. S. Biswas and P. Van Der Voort, *Eur. J. Inorg. Chem.*, 2013, **2013**, 2154-2160.
50. M. R. DeStefano, T. Islamoglu, S. J. Garibay, J. T. Hupp and O. K. Farha, *Chem. Mater.*, 2017, **29**, 1357-1361.
51. H. Noh, C.-W. Kung, T. Islamoglu, A. W. Peters, Y. Liao, P. Li, S. J. Garibay, X. Zhang, M. R. DeStefano, J. T. Hupp and O. K. Farha, *Chem. Mater.*, 2018, **30**, 2193-2197.
52. Z. Hu, Y. Peng, Z. Kang, Y. Qian and D. Zhao, *Inorg. Chem.*, 2015, **54**, 4862-4868.
53. H. Reinsch, B. Bueken, F. Vermoortele, I. Stassen, A. Lieb, K.-P. Lillerud and D. De Vos, *CrystEngComm*, 2015, **17**, 4070-4074.
- C. Avci-Camur, J. Perez-Carvajal, I. Imaz and D. MasPOCH, *ACS Sustain Chem Eng.*, 2018, **6**, 14554-14560.
55. S. Waitschat, H. Reinsch and N. Stock, *Chem. Commun.*, 2016, **52**, 12698-12701.
56. P. A. Julien, C. Mottillo and T. Friščić, *Green Chem.*, 2017, **19**, 2729-2747.
57. Z. Hu, I. Castano, S. Wang, Y. Wang, Y. Peng, Y. Qian, C. Chi, X. Wang and D. Zhao, *Cryst. Growth Des.*, 2016, **16**, 2295-2301.
58. D. Britt, D. Tranchemontagne and O. M. Yaghi, *Proc. Natl. Acad. Sci. U.S.A.*, 2008, **105**, 11623.
59. G. W. Peterson, J. B. DeCoste, F. Fatollahi-Fard and D. K. Britt, *Ind. Eng. Chem. Res.*, 2014, **53**, 701-707.
60. H. Jasuja, G. W. Peterson, J. B. Decoste, M. A. Browe and K. S. Walton, *Chem Eng Sci*, 2015, **124**, 118-124.
61. Y. Khabzina and D. Farrusseng, *Microporous Mesoporous Mater.*, 2018, **265**, 143-148.
62. C. Petit and T. J. Bandoz, *Adv. Funct. Mater.*, 2009, **20**, 111-118.
63. J. F. Van Humbeck, T. M. McDonald, X. Jing, B. M. Wiers, G. Zhu and J. R. Long, *J. Am. Chem. Soc.*, 2014, **136**, 2432-2440.
64. A. J. Rieth, Y. Tulchinsky and M. Dincă, *J. Am. Chem. Soc.*, 2016, **138**, 9401-9404.
65. G. Barin, G. W. Peterson, V. Crocellà, J. Xu, K. A. Colwell, A. Nandy, J. A. Reimer, S. Bordiga and J. R. Long, *Chem. Sci.*, 2017, **8**, 4399-4409.
66. A. J. Rieth and M. Dincă, *J. Am. Chem. Soc.*, 2018, **140**, 3461-3466.
67. J. N. Joshi, E. Y. Garcia-Gutierrez, C. M. Moran, J. I. Deneff and K. S. Walton, *J. Phys. Chem. C*, 2017, **121**, 3310-3319.
68. Y.-C. Yang, *Acc. Chem. Res.*, 1999, **32**, 109-115.
69. S.-Y. Moon, E. Proussaloglou, G. W. Peterson, J. B. DeCoste, M. G. Hall, A. J. Howarth, J. T. Hupp and O. K. Farha, *Chem. Eur. J.*, 2016, **22**, 14864-14868.
70. S.-Y. Moon, G. W. Wagner, J. E. Mondloch, G. W. Peterson, J. B. DeCoste, J. T. Hupp and O. K. Farha, *Inorg. Chem.*, 2015, **54**, 10829-10833.
71. F. Yang, H. Huang, X. Wang, F. Li, Y. Gong, C. Zhong and J.-R. Li, *Cryst. Growth Des.*, 2015, **15**, 5827-5833.
72. M. J. Cliffe, W. Wan, X. Zou, P. A. Chater, A. K. Kleppe, M. G. Tucker, H. Wilhelm, N. P. Funnell, F.-X. Coudert and A. L. Goodwin, *Nat. Commun.*, 2014, **5**, 4176.
73. T. Islamoglu, D. Ray, P. Li, M. B. Majewski, I. Akpınar, X. Zhang, C. J. Cramer, L. Gagliardi and O. K. Farha, *Inorg Chem*, 2018, **57**, 13246-13251.
74. T. Grant Glover, G. W. Peterson, B. J. Schindler, D. Britt and O. Yaghi, *Chem Eng Sci*, 2011, **66**, 163-170.
75. J.-W. Lee, G. Barin, G. W. Peterson, J. Xu, K. A. Colwell and J. R. Long, *ACS Appl. Mater. Interfaces*, 2017, **9**, 33504-33510.
76. A. X. Lu, M. McEntee, M. A. Browe, M. G. Hall, J. B. DeCoste and G. W. Peterson, *ACS Appl. Mater. Interfaces*, 2017, **9**, 13632-13636.
77. T. J. Bandoz, M. Laskoski, J. Mahle, G. Mogilevsky, G. W. Peterson, J. A. Rossin and G. W. Wagner, *J. Phys. Chem. C*, 2012, **116**, 11606-11614.

## Table of Contents

